Identification of novel mutations in Japanese ovarian clear cell carcinoma patients using optimized targeted NGS for clinical diagnosis

（臨床診断に向けたターゲットシーケンスによる卵巣明細胞癌患者の変異解析）

千葉大学大学院医学薬学府

先端医学薬学専攻

（主任：永瀬　浩喜 教授）

丸　喜明

CONTENTS

1. ABSTRACT ··· **1**

2. INTRODUCTION ··· **3**

3. MATERIALS AND METHODS ··· **6**

3.1. Patients and pathological materials ··· 6

3.2. The quality assessment of DNA extracted from FFPE samples ··· 7

3.3. Library preparations ··· 8

3.4. Emulsion PCR and enrichment ··· 9

3.5. Sequencing and mutation analysis ··· 9

3.6. Identification of somatic variants ···10

3.7. Validation using Sanger sequencing ···10

4. RESULTS **…11**

4.1. Eighteen pairs of DNA from FFPE samples passed quality check …11

4.2. Clinico-pathological features of 18 cases …11

4.3. Forty five out of 92 candidate somatic mutations were detected …12

4.4. Characteristics of somatic mutations in 18 Japanese OCCCs …13

4.5. Eleven known somatic mutations and 7 novel somatic mutations were identified across 7 genes that harbor somatic mutations in multiple OCCC cases …14

4.6. NGS analyses using FFPE and FF samples demonstrated highly concordant results …15

4.7. Tumor heterogeneity was uncovered by FFPE-based NGS analysis …16

5. DISCUSSION **…17**

6. ACKNOWLEDGEMENTS **…23**

7. REFERENCES **…24**

8. TABLES

Table 1 Clinico-pathologic features of enrolled 29 OCCC cases and 18 cases which passed DNA quality control testing …31

Table 2 Clinico-pathologic features of 29 OCCCs and summary of somatic mutations identified from 18 OCCCs sequenced by the NGS analysis …32

Table 3 A total of 7 genes were mutated in multiple OCCC cases …33

Table 4 Summary of 45 somatic mutations in 34 genes were identified in 18 OCCCs …34

9. FIGURES **⋯35**

Figure 1 Representative images of OCCC for this study ⋯35

Figure 2 A dot blot of the distribution of quality of each DNA sample extracted from FFPE samples of 29 cases ⋯36

Figure 3 Validation by Sanger sequencing and filtering of NGS data for candidate somatic mutations ⋯37

Figure 4 A summary of 45 somatic mutations identified by NGS analysis for 409 cancer-related genes in 18 OCCC samples ⋯38

Figure 5 A comparative representations between FFPE and FF-based NGS from three OCCC cases ⋯39

Figure 6 Variable histological features of OCCC cases ⋯40

1. ABSTRACT

Objective. Ovarian clear cell carcinoma (OCCC) is an aggressive ovarian cancer with a higher frequency in Japan and often becomes chemorefractory disease. Reliable genetic diagnosis is essential to affirm the success of precision medicine for OCCC treatment. The aim of this study is, therefore, to identify novel mutations in OCCCs and develop a feasible clinical next generation sequencing (NGS) approach using formalin-fixed paraffin-embedded (FFPE) rather than preferable but not always available fresh frozen (FF) samples.

Methods. We optimized and evaluated exome analyses of 409 cancer-related genes using FFPE and FF DNA and analyzed NGS data to identify somatic mutations in Japanese OCCCs.

Results. Sufficient and good quality DNAs from FFPE samples were extracted from 18 (FIGO Stage I: 12) out of 29 pairs of matched normal and OCCC for NGS (63%). The fine quality of extracted DNAs depended on the length of storage period (less than 2 years storage was better quality). We also identified 45 somatic mutations in 34 genes including unreported variants from those FFPE DNA, in which somatic mutations in the PIK3CA gene were the most common (28%) as previously reported. Seven genes (*PIK3CA*, *ARID1A*, *CTNNB1*, *CSMD3*, *LPHN3*, *LRP1B*, and *TP53*) were

mutated in at least two independent OCCCs. *CSMD3*, *LPHN3*, and *LRP1B* have not been reported in OCCC. FF samples from 3 out of those 18 OCCCs were available and 13 out of 14 FFPE somatic mutations were concordant.

Conclusions. We successfully identified novel genetic alterations in Japanese OCCCs and demonstrated a feasible clinical diagnostic procedure using targeted NGS for OCCC FFPE samples.

Key words: Somatic mutations, Next-generation sequencing, Clinical sequencing, FFPE, Ovarian clear cell carcinoma.

2. INTRODUCTION

Ovarian carcinoma (OC) is the most devastating malignant gynecological tumors. In the United States, 21,290 new cases and 14,180 deaths were estimated in 2015 [1]. Hence, it has been dubbed the “Silent Killer”, since it is difficult to diagnose and treat in its early stage due to the lack of obvious symptoms. Although many surgical techniques and chemotherapies have been developed, 5 year survival rate for OC is 44% [2, 3].

About 90% of primary OCs are epithelial carcinomas and are divided into 4 major histological types: serous, mucinous, endometrioid, and clear cell. Recently, ovarian epithelial carcinoma is classified into 2 broad simplified categories. Type I includes low-grade serous, endometrioid, clear cell, mucinous, and transitional cell carcinomas based on the histopathology and genomic studies, while high-grade serous carcinomas, undifferentiated carcinomas, and carcinosarcomas belong type II [4]. Ovarian clear cell carcinoma (OCCC) is the type I tumor, but nevertheless showed unfavorable prognosis when diagnosed at an advanced stage because of poor response rates to platinum-based chemotherapy [5, 6]. There is a considerable geographical variation in OCCC incident rates and prevalence; 1-12% of OC in Europe and the United States is OCCC, while 15-25% in Japan [4, 7-9]. Endometriosis is a risk factor

for OCCC. Nevertheless, OCCCs do not express estrogen or progesterone receptors, therefore a hormone independent during the transformation process. [9] Although little is known about the pathogenesis of OCCC, frequent somatic mutations of the *AT rich interactive domain 1A* (*SWI-like*) (*ARID1A*) [10, 11] and *phosphatidylinositol-4, 5-bisphosphate 3-kinase, catalytic subunit alpha* (*PIK3CA*) genes [12] have been reported. Cancer therapy continues its shift towards molecular target agents and increasingly individually tailored regimens. Therefore patient's precise genetic information is increasingly important for individualized treatment toward 'precision medicine'. Recent advances in next-generation sequencing (NGS) allow cancer patients to gain access to the genetic profiling of their cancers and to identify many novel mutations including actionable therapeutic targets.

DNA extracted from fresh frozen (FF) samples is generally used for NGS analysis for genetic profiling of cancer and provides a typically high quality DNA fragments for NGS sequencing. However, FF samples may not be available for all cancer patients, while formalin-fixed paraffin-embedded (FFPE) samples are currently the most widely available specimen for general clinical set-ups besides cost-effectiveness. Furthermore FFPE samples along with histopathological evaluation allow to analyze intra-tumor genetic diversity and tumor heterogeneity. One major

limitation to use DNA from routinely prepared FFPE samples may be a poor quality of the extracted DNA comparing with FF samples, which is more suitable for basic research. NGS analysis using FFPE samples have been reported successfully in gastrointestinal tract [13], bladder [14], prostate [15], and lung [16] cancers.

Herein, we successfully optimized each step condition for FFPE-based NGS procedures targeting 409 cancer-related genes and showed analogous results between the analyses using the FFPE and the FF. We detected known somatic mutations, as well as some novel mutations, and its intratumoral genetic heterogeneity, confirming the reasonable compatibility with previous studies, although there exist ethnic/racial disparities in the prevalence of OCCC.

3. MATERIALS AND METHODS

3.1. Patients and pathological materials

This study was approved by the ethics committee of the Chiba Cancer Center, Chiba, Japan (Institutional Review Board approval number 24-92). Twenty nine patients with histologically confirmed OCCC were used from archives in the division of surgical pathology in Chiba Cancer Center (Table 1). None of them had undergone chemotherapy or radiation therapy before surgery. Adequate FFPE blocks that contain sufficient amount of cancer cells in pathological specimens confirmed by the Hematoxylin & Eosin stain and immunohistochemical stainings were selected before the tissue dissection. Ten FFPE serial sections of 6 μm thickness per sample for tumor and normal tissues were used. However, many FFPE samples exhibit high degrees of tumor heterogeneity, with varied admixture of reactive stroma, inflammatory cells and necrosis. We performed macrodissection to enrich tumor cells on FFPE serial sections (> 80% tumor cells) (Figure 1). Furthermore FF samples from 3 patients were available and subjected to NGS analysis to assess the feasibility of FFPE-based NGS.

3.2. The quality assessment of DNA extracted from FFPE samples

DNA was extracted from FFPE samples using the QIAmp DNA FFPE Tissue Kit (Qiagen, Hilden, Germany) according to the manufacturer's instructions. Quality and quantity of DNA were assessed using Nano-Drop ND-1000 Spectrophotometer (Nano Drop Technologies, Wilmington, DE), agarose gel electrophoresis and quantitative polymerase chain reactions (qPCR). qPCR was conducted with 5 ng and 20 ng of template DNAs using the FFPE DNA QC Assay (Thermo Fisher Scientific, Waltham, Massachusetts, USA). Briefly, a 256 bp fragment DNA was amplified by PCR using forward primer of 5'-AGCTGAGTGCGTCCTGTCACT-3' and reverse primer of 5'-ACCTCACCTCAGCCATTGAACT-3' adding Taq Man Gene Expression Master Mix (Thermo Fisher Scientific) according to the manufacturer's instructions. TaqMan MGB Probe (FAM) used was 5'-CACTCCCATGTCCC-3'. If after determination of DNA amount measured by Nano-Drop-1000 Spectrophotometer either 5 ng or 20 ng of template DNAs passed quality assessment by qPCR (the cut-off value of > 0.3), the NGS analysis was performed. This cut-off value was determined by our previous experiments that relative value of > 0.3 resulted in successful NGS analysis (unpublished data).

3.3. Library preparations

Library preparation for the 409 gene panel was performed using the Ion AmpliSeq™ Comprehensive Cancer Panel (CCP) (Thermo Fisher Scientific). The panel was designed to facilitate targeted amplification-based capture and sequencing of coding regions of 409 cancer-related genes. It includes 4 primer pools with approximately 4000 primer pairs in each pool and requires a total of 40-80 ng of DNA as a template for each sample (10-20 ng per pool) in this study. Library preparations for each sample were performed using the CCP, the Ion Ampliseq™ Library Kit 2.0-96LV, the Ion Xpress Barcode Adaptors 1-96 Kit (Thermo Fisher Scientific), and the Agencourt AMPure XP reagent (BD Biosciences, Franklin Lakes, NJ, USA). The library was then quantified using the Ion Library Quantitation Kit (Thermo Fisher Scientific). On the basis of these results, the library was diluted to 8 pM.

3.4. Emulsion PCR and enrichment

The clonal amplification of barcoded DNA library onto ion spheres (ISPs) was carried out using emulsion PCR (Ion PI™ Template OT2 Kit v3) in the Ion One Touch™ 2 instrument (Thermo Fisher Scientific). Ratio of imputed library of tumor to normal was set at 3 to 1 (simultaneously 3 pairs in 1 run). Following emulsion PCR and recovery, isolation of amplified templates on ISPs was performed using the Ion One Touch™ ES (Thermo Fisher Scientific).

3.5. Sequencing and mutation analysis

Targeted sequencing of 409 cancer-related genes was performed on ion torrent Ion Proton sequencer (Thermo Fisher Scientific). Briefly, the barcoded libraries were loaded into the Ion PI™ Chip v2 (3 samples per chip) using the Ion PI™ Sequencing 200 Kit v3 according to manufacturer's instructions. Subsequently, the Ion PI™ chip was analyzed by Ion Proton sequencer. The Torrent Suite software was used to parse a barcoded read, to align to the human reference genome (hg19), and to generate run metrics, including chip loading efficiency, total read counts, and quality. Variant Caller v4.0.2 software was used for variant detection. All variants were annotated ANNOVAR.

3.6. Identification of somatic variants

A number of steps were used to filter nucleotide variants identified in the screening; (1) nonsynonymous and nonsense single nucleotide variants and (2) tumor specific somatic mutations with variant allele frequencies of > 10%. Furthermore variants were observed using the Integrated Genomics Viewer, which can visualize the read alignment and the presence of variants to exclude sequencing errors.

3.7. Validation using Sanger sequencing

Somatic mutations with variant allele frequencies > 15% were validated using the Sanger sequencing method account for primer setting and performance of Sanger sequencing. Sanger sequencing was performed on an Applied Biosystems 3730 DNA analyzer (Applied Biosystems, Foster City, CA, USA) and sequences were analyzed with Sequencing Analysis software 6 (Applied Biosystems).

4. RESULTS

4.1. Eighteen pairs of DNA from FFPE samples passed quality check

DNA was extracted from 58 FFPE blocks of 29 cases diagnosed with OCCC. Details of the storage period of the FFPE block were as follows: 36-48 months in 1 cases, 24-36 months in 8 cases, 12-24 months in 5 cases, and 1-12 months in 15 cases. DNAs extracted from those FFPE samples were checked by a standard qPCR procedure creating a 256 bp product. DNA quality of each paired sample was similar. Eighteen cases (63%) passed a quality check of relative value 0.3. DNA extracted from FFPE samples preserved for a shorter time period showed better quality. Eighteen cases: 1 out of 8 cases for the storage period of 24-36 months, 4 of 5 cases for 12-24 months, and 13 out of 15 cases for 1-12 months, passed the quality check and were subjected to the subsequent NGS analysis. In terms of fixation time, 40% of cases fixed for over 24 h passed quality, while 67% for < 24 h passed (Figure 2, Table 2).

4.2. Clinico-pathological features of 18 cases

Of 18 cases (range, 41 to 71 years and Median 55), all are unilateral ovarian tumors (nine right, nine left) and 16 were diagnosed with clear cell adenocarcinoma, 1 was clear cell adenocarcinofibroma, and 1 was mixed epithelial tumor (clear cell and

endometrioid adenocarcinoma). The international clinical staging system by Federation of Gynecology and Obstetrics (FIGO) was used and 12 cases were diagnosed stage I (66%); 3 for stage II (17%); 2 for stage III (11%); and 1 for stage IV (6%). Thirteen out of 18 cases (72%) manifested endometoriosis (Table.1).

4.3. Forty five out of 92 candidate somatic mutations were detected

A total of 92 candidate somatic mutations in 65 genes with variant allele frequencies of > 10% were identified from 18 OCCCs by NGS analysis. We performed validation by Sanger sequencing for 58 of them with variant allele frequencies of > 15%. Forty (69%) of these 58 somatic mutations were concordant between NGS and Sanger sequencing. The rest of 18 discordant somatic mutations fall in two categories; (1) number of coverage reads of normal tissues was < 20 reads, (2) number of coverage reads of normal tissues was > 20 reads but distance from amplicon boundaries to variant position was < 6 bp (Figure 3a). Thus we optimized the filtering of NGS data as follows: coverage of normal tissue is > 20 reads and amplicon boundaries from the variant is > 6 bp. After applying this filtering of the somatic mutations with variant allele frequencies of 10 to 15%, 5 somatic mutations were filtering out (Figure 3b).

Finally, a total of 45 somatic mutations in 34 genes were considered to be somatic mutations in OCCCs.

4.4. Characteristics of somatic mutations in 18 Japanese OCCCs

Average number of somatic mutations identified in each tumor was 2.5 alterations (range, 1 to 6). A total of 7 genes were mutated in multiple OCCC cases: 5 in *PIK3CA* (28%), 3 in *ARID1A*, and 2 in *catenin, beta 1* (*CTNNB1*), *CUB and Sushi multiple domains 3* (*CSMD3*), *latrophilin 3* (*LPHN3*), *low-density lipoprotein receptor related protein 1B* (*LRP1B*), or *tumor protein p53* (*TP53*). The number of mutations in each case was not associated with FIGO staging, age and endometriosis. C to T transition was the most frequent substitution mutations in 45 somatic mutations (Figure 4). Furthermore functional analysis by GeneMANIA identified 83 functions using the false discovery rate of < 0.05. Among these, the top 5 functions were phosphatidylinositol 3-kinase (PI3K) activity/phosphatidylinositol-mediated pathway (mutated in 6 cases, 33% [*PIK3CA*, *v-erb-b2 avian erythroblastic leukemia viral oncogene homolog 2* (*ERBB2*), *phosphatidylinositol-4,5-bisphosphate 3-kinase catalytic subunit gamma* (*PIK3CG*), *phosphoinositide-3-kinase regulatory subunit 2* (*PIK3R2*), *phosphatase and tensin homolog* (*PTEN*)]), fibroblast growth factor receptor signaling

pathway (8 cases, 44% [*PIK3CA*, *CTNNB1*, *ERBB2*, *PIK3R2*, *PTEN*, *protein phosphatase 2, regulatory subunit A, alpha* (*PPP2R1A*)]), chromatin remodeling (3 cases, 17% [*ARID1A*, *SWI/SNF related, matrix associated, actin dependent regulator of chromatin, subfamily a, member 4* (*SMARCA4*)]), Fc receptor signaling pathway (6 cases, 33% [*PIK3CA*, *ERBB2*, *PIK3R2*, *PTEN*, *wiskott-aldrich syndrome* (*WAS*)]), and epidermal growth factor receptor signaling pathway (6 cases, 33% [*PIK3CA*, *ERBB2*, *F-box and WD repeat domain containing 7, E3 ubiquitin protein ligase* (*FBXW7*), *PIK3R2*, *PTEN*]) pathways. At least one of each aberration of these five functions was seen in 12 out of 18 OCCCs (67%).

4.5. Eleven known somatic mutations and 7 novel somatic mutations were identified across 7 genes that harbor somatic mutations in multiple OCCC cases

Three somatic mutations of *ARID1A* were nonsense mutations (p.Q464X, p.Q566X, and p.Q601X). Fifteen non-synonymous mutations in 6 genes were further analyzed for functional prediction of amino acid changes using the Protein Variation Effect Analyzer (PROVEAN). PROVEAN Genome Variants of PROVEAN tool calculates PROVEAN-score (cut-off=-2.5) and SIFT-score (cut-off=0.05). Eight out of 15 mutations were evaluated to deleterious in PROVEAN and damaging in SIFT. In

these 15 somatic mutations, 9 mutations were reported in the Catalogue of Somatic Mutations in Cancer (COSMIC) database: *PIK3CA* (p.M1004I, p.E545G. p.H1047R, p.E542K, and p.V346G), *CTNNB1* (p.S33C and p.S37C), *TP53* (p.R43H and p.E11K) and some were overlapping with functional prediction. Six somatic mutations were found in the Single Nucleotide Polymorphism Database (dbSNP): *PIK3CA* (p.E545G, p.H1047R, and p.E542K), *CTNNB1* (p.S33C and p.S37C), *TP53* (p.R43H). Out of 7 somatic mutations that were not previously enrolled in COSMIC database or dbSNP, 5 mutations affecting *CSMD3* (p.R1021H and p.L1828V), *LPHN3* (p.E223K and p.L1039I) and *ARID1A* (p.Q601X) were predicted to alter physiological function of the gene products, while the other 2 mutations affecting *LRP1B* (p.I2759M and p.R151K) were not (Table 3).

4.6. NGS analyses using FFPE and FF samples demonstrated highly concordant results

NGS analyses using 3 paired FFPE and FF samples under our optimized conditions demonstrated highly concordant results (93%). Not only identified genes but also variant allele frequency was similar between two analyses. On the other hand,

somatic mutation of *APC membrane recruitment protein 1* (*AMER1*) was only identified from FFPE sample #12, but not in FF analysis of the same sample (Figure 5).

4.7. Tumor heterogeneity was uncovered by FFPE-based NGS analysis

To verify tumor heterogeneity by FFPE-based NGS, we compared histologically distinct lesions in the same patient. Of 2 lesions with variable morphologies of OCCC, one lesion was composed of tumor cells with abundant basement membrane like material and harbored *CTNNB1* (p.S37C) mutation, while the other region was solid growth pattern and harbored *CTNNB1* (p.S37C) as well as *LPHN3* mutation (p.E223K) (Figure 6a, b). In a case of mixed epithelial tumors, 2 somatic mutations of *CTNNB1* (p.S33C) and *p21 protein* (*Cdc42/Rac*)-*activated kinase 3* (*PAK3*) (p.P517S) were identified in both clear cell adenocarcinoma and endometrioid adenocarcinoma components, whereas somatic mutation of *TP53* (p.R43H) was identified only in clear cell adenocarcinoma component (Figure 6c, d). The *AMER1* mutation only in FFPE sample #12 could also indicate tumor heterogeneity (Figure 5).

5. DISCUSSION

In our best knowledge, this is the first report of a comprehensive mutation search on Japanese FFPE OCCC samples using semiconductor sequencer (Ion Proton) targeting 409 cancer related genes. DNA extracted from short-term stored FFPE samples (< 2 years) was generally feasible for NGS. Effect of length of the storage period of FFPE is however controversial. Schwiger et al. reported that it is a minor influence on sequencing quality [17], while Hedegaard et al. reported that longer storage time resulted in a decreased fraction of mapped reads, increased fraction of non-perfectly mapped reads and reads mapping with unaligned ends [18]. Our results suggested that the storage time of FFPE samples has been influenced on quality of DNA and NGS analysis. Although storage conditions (temperature, humidity and exposure of sun or light) of FFPE samples might affect, basic clinical set up of our examined procedure without any special process for molecular analysis, therefore, can be applied any standard hospitals. Furthermore, we suggested that desirable fixation time could be < 24 h. Candidate somatic mutations identified by NGS analysis were confirmed by Sanger sequencing and/or optimized filtering to minimize false positive calls. The filtering from all variants calls in NGS data is practical avoiding time-consuming and expensive processes of Sanger sequencing validation. Although such a FFPE-based

NGS is needed for clinical settings of certain hospitals, of course, accreditation is important for clinical application and certification of International Organization for Standardization should be applied to clinical sequencing.

The most frequent mutated gene identified in this study was the *PIK3CA* gene (28%: 5/18), which encodes the catalytic subunit p110a of PIK3 and is located on chromosome 3q26.3. Both somatic mutations and gene amplification of *PIK3CA* increase PI3K activity and activate the downstream Akt signaling pathway. Kuo, et al. showed that somatic activating mutations *PIK3CA* were frequently observed in OCCC (33%) [12]. Furthermore we identified somatic mutations of *PIK3CG*, a class I catalytic subunit of PI3K and PIK3R2, class IA PI3K regulatory isoforms. The other six multiple mutated genes (*ARID1A*, *CTNNB1*, *CSMD3*, *LPHN3*, *LPR1B*, and *TP53*) were identified. *ARID1A* is a key component of the SWI/SNF chromatin-remodeling complex that is conserved in all eukaryotes, plays important role in controlling gene expression and is critical in development, differentiation, and tumor suppression [19]. Although 46% and 57% of frequent somatic mutations of *ARID1A* in OCCC have been published recently by whole-transcriptome and exome sequencing analyses, respectively [10, 11], it was 17% in this study. Mutation of SWI/SNF related gene *SMARCA4* was identified in one case, hence other genes in the ARID1 pathway may be mutated in the rest of

cases. Coexistence of *PIK3CA* and *ARID1A* mutations has been reported to contribute to ovarian clear cell tumorigenesis [20, 21], whilst it was only one case in this study. These differences might be explained by several factors such as tumor heterogeneity, sequencing methods, and enrolled population. Recently, Er TK, et al. reported that the most frequently mutated genes in 10 Taiwanese endometriosis-associated ovarian cancer (EAOC) patients were *PIK3CA* (6/10) and *ARID1A* (5/10) by the same deep sequencing method. In this study, 8 OCCCs were analyzed and found *PIK3CA* (4/8) and *ARID1A* (4/8) mutations [22] and discussed one hypermutated phenotype. We found the mutation frequency of *PIK3CA* and *ARID1A* in EAOC cases was 3/13 and 3/13, respectively. This can be partially explained by no hypermutated phenotype in this study. *CTNNB1* mutation was observed in a mixed epithelial tumor patient (clear cell adenocarcinoma and endometrioid carcinoma). McConechy, et al. showed that frequency of *CTNNB1* mutations is 53% in low-grade ovarian endometrioid carcinoma [23]. Endometriosis is associated with the development of ovarian low-grade endometrioid carcinoma and also plays an important role in risk and pathogenesis of OCCC [24, 25]. *TP53*, one of the most frequently mutated genes in carcinoma, was also mutated in OCCC [26]. Clear cell carcinomas can arise in the ovary and the uterus, and show histological and biological similarities across sites. There are, however, some apparent differences between OCCC

and endometrial clear cell carcinoma (ECCC). Based on previous reports, *ARID1A* protein loss and *PIK3CA* mutations are observed in approximately 23% and 9% of ECCC, respectively [27, 28]. PI3K/AKT/mTOR signaling and chromatin remodeling pathways must be major functional pathways of OCCC carcinogenesis [29], which is also observed in this study. Somatic mutations of *CSMD3*, *LPHN3*, and *LRP1B* have not been reported in OCCC, which have been associated with tumorigenesis and chemoresistance. Thus, further functional analysis including recent advances of organoid and gene editing technologies shall be needed to identify the functional role of those mutation on OCCC carcinogenesis [30-33]. Genetic diagnosis of OCCC is also important to select molecular targeted therapies, such as mTOR inhibitor [34] and synthetic lethality of *ARID1A* [35].

Recent reports suggested that not only pathway signature but also mutation signature is important to recapitulate carcinogenesis in individual cancer [36]. Our results showing C to T transition was most frequently observed (53.3%) as seen in the type 1B category and interestingly, type 3 next to type 1B is associated with *breast cancer 1/2, early onset* (*BRCA1/2*) mutations. Because high-grade serous adenocarcinoma is associated with *BRCA1/2* mutations and the expression profile of high-grade serous adenocarcinoma differ from the expression profile of OCCC [37, 38],

type 3 might correspond to high-grade serous adenocarcinoma. Although there have been reported that formalin fixation associated with artificial C to T transition and might make a bias of subsequent sequencing results [39, 40], there was almost no difference in the frequency of C to T transitions between FF- and FFPE-based NGS data. Although a T to G substitution mutation, not C to T transitions, in the *AMER1* gene was identified only from FFPE sample, this is unlikely to be artificial but rather reflects tumor heterogeneity. Therefore, FFPE samples showed high concordance with FF samples. For better understanding of tumor heterogeneity, detailed analysis of histomorphology, immunophenotype, and genetic alterations from multiple legions should be employed to perform the companion diagnosis to treat, care and/or manage each OCCC patient. In this respect, genetic analysis from FFPE samples is a suitable approach to understand tumor heterogeneity of patients [13-15]. We also showed mutational heterogeneity within a tumor using DNAs obtained from different dissected samples.

In summary, we successfully established an optimized clinical molecular diagnosis procedure in OCCC using FFPE-based NGS of 409 cancer-related genes and identified 45 somatic mutations in 34 genes in Japanese women (Table 4, Figure 4). Not only pathological diagnosis but also subclassification of OCCC based on a large-scale analysis of genetic variation and biological function prediction is essential for

adequately predicting response to therapy in patients, its tumor behavior, origin, and carcinogenesis. Although further improvement of FFPE-based NGS methods are required, clinical sequencing using FFPE samples which is widely used pathological diagnosis will be a powerful and essential tool for clinical molecular diagnosis in medical diagnostic laboratories.

6. ACKNOWLEDGMENTS

The author is especially grateful to Hiroki Nagase, Naotake Tanaka, Miki Ohira, Makiko Itami, and Yoshitaka Hippo for experimental planning and helpful discussion.

The author thanks members of Laboratory of Cancer Genomics of Chiba Cancer Center Research Institute for their kind supports to perform next generation sequencing and Sanger sequencing.

The author also thanks members of Department of Surgical Pathology of Chiba Cancer Center for pathological diagnosis.

This work is supported by JSPS KAKENHI Grant-in-Aid for Scientific Research on Innovative Areas Grant Number JP26112517, JP25134718, JP16H01579 and Grant-in-Aid for Scientific Research (B) Grant Number JP26290060.

7. REFERENCES

[1] R.L. Siegel, K.D. Mller, A. Jemal, Cancer statistics, 2015, CA Cancer J. Clin. 65 (2015) 5–29.

[2] M.P. Coleman, D. Forman, H. Bryant, J. Butler, B. Rachet, C. Maringe, et al., Cancer survival in Australia, Canada, Denmark, Norway, Sweden, and UK, 1995–2007 (the International Cancer Benchmarking Partnership): an analysis of population-based cancer registry data, Lancet 377 (2011) 127–138.

[3] R. Siegel, J. Ma, Z. Zou, A. Jemal, Cancer statistics, 2014, CA Cancer J. Clin. 64 (2014) 9–29.

[4] M. Koshiyama, N. Matsumura, I. Konishi, Recent concepts of ovarian carcinogenesis: type 1 and type 2, Biomed. Res. Int. 2014 (2014) 934261.

[5] T. Sugiyama, T. Kamura, J. Kigawa, N. Terakawa, Y. Kikuchi, T. Kita, et al., Clinical characteristics of clear cell carcinoma of the ovary: a distinct histologic type with poor prognosis and resistance to platinum—based chemotherapy, Cancer 88 (2000) 2584–2589.

[6] H. Itamochi, J. Kigawa, N. Terakawa, Mechanisms of chemoresistance and poor prognosis in ovarian clear cell carcinoma, Cancer Sci. 99 (2008) 653–658.

[7] K. Ushijima, Current status of gynecologic cancer in Japan, J. Gynecol. Oncol. 20

(2009) 67–71.

[8] R.A. Soslow, Histologic sybtypes of ovarian carcinoma: an over view, Int. J. Gynecol. Pathol. 27 (2008) 161–174.

[9] C.L. Pearce, C. Templeman, M.A. Rossing, A. Lee, A.M. Near, P.M. Webb, et al., Association between endometriosis and risk of histological subtypes of ovarian cancer: pooled analysis of case-control studies, Lancet Oncol. 13 (2012) 385–394.

[10] K.C. Wiegand, S.P. Shah, O.M. Al-Agha, Y. Zhao, K. Tse, T. Aeng, et al., ARID1A mutations in endometriosis-associated ovarian carcinomas, N. Engl. J. Med. 363 (2010) 1532–1543.

[11] S. Jones, T.L. Wang, I.M. Shih, T.L. Mao, K. Nakayama, R. Roden, et al., Frequent mutations of chromatin remodeling gene ARID1A in ovarian clear cell carcinoma, Science 330 (2010) 228–231.

[12] K.T. Kuo, T.L. Mao, S. Jones, E. Veras, A. Ayhan, T.L. Wang, et al., Frequent activating mutations of PIK3CA in ovarian clear cell carcinoma, Am. J. Pathol. 174 (2009) 1597–1601.

[13] A. Mafficini, E. Amato, M. Fassan, M. Simbolo, D. Antonello, C. Vicentini, et al., Reporting tumor molecular heterogeneity in histopathological diagnosis, PLoS One 9 (2014), e104979.

[14] J.I. Warrick, D.H. Hovelson, A. Amin, C.J. Liu, A.K. Cani, A.S. McDaniel, et al., Tumor evolution and progression in multifocal and paired non-invasive/invasive urothelial carcinoma, Virchows Arch. 466 (2015) 297–311.

[15] H. Beltran, R. Yelensky, G.M. Frampton, K. Park, S.R. Downing, T.Y. MacDonald, et al., Targeted next-generation sequencing of advanced prostate cancer identifies potential therapeutic targets and disease heterogeneity, Eur. Urol. 63 (2013) 920–926.

[16] I.S. Hagemann, S. Devarakonda, C.M. Lockwood, D.H. Spencer, K. Guebert, A.J. Bredemeyer, et al., Clinical next-generation sequencing in patients with non-small cell lung cancer, Cancer 121 (2015) 631–639.

[17] M.R. Scweiger, M. Kerick, B. Timmermann, M.W. Albrecht, T. Borodina, D. Parkhomchuk, et al., Genome-wide massively parallel sequencing of formaldehyde fixed-paraffin embedded (FFPE) tumor tissues for copy-number- and mutation-analysis, PLoS One 4 (2009), e5548.

[18] J. Hedegaard, K. Thorsen, M.K. Lund, A.M. Hein, S.J. Hamilton-Dutoit, S. Vang, et al., Next-generation sequencing of RNA and DNA isolated from paired fresh-frozen and formalin-fixed paraffin-embedded samples of human cancer and normal tissue, PLoS One 9 (2014), e98187.

[19] B.G. Wilson, C.W. Roberts, SWI/SNF nucleosome remodelers and cancer, Nat. Rev.

Cancer 11 (2011) 481–492.

[20] S. Yamamoto, H. Tsuda, M. Takano, S. Tamai, O. Matsubara, Loss of ARID1A protein expression occurs as an early event in ovarian clear-cell carcinoma development and frequently coexists with PIK3CA mutations, Mod. Pathol. 25 (2012) 615–624.

[21] R.L. Chandler, J.S. Damrauer, J.R. Raab, J.C. Schisler, M.D. Wilkerson, J.P. Didion, et al., Coexistent ARID1A-PIK3CA mutations promote ovarian clear-cell tumorigenesis through pro-tumorigenic inflammatory cytokine signaling, Nat. Commun. 6 (2015) 6118.

[22] T.K. Er, Y.F. Su, C.C. Wu, C.C. Chem, J. Wang, T.H. Hsieh, et al., Targeted next-generation sequencing for molecular diagnosis of endometriosis-associated ovarian cancer, J. Mol. Med. 94 (2016) 835–847.

[23] M.K. McConechy, J. Ding, J. Senz, W. Yang, N. Melnyk, A.A. Tone, et al., Ovarian and endometrial endometrioid carcinomas have distinct CTNNB1 and PTEN mutation profiles, Mod. Pathol. 27 (2014) 128–134.

[24] R.J. Kurman, L.M. Shih, The origin and pathogenesis of epithelial ovarian cancer-proposed unifying theory, Am. J. Surg. Pathol. 34 (2010) 433–443.

[25] H. Kajihara, Y. Yamada, H. Shigetomi, Y. Higashiura, H. Kobayashi, The dichotomy in the histogenesis of endometriosis-associated ovarian cancer: clear

cell-type versus endometrioid-type adenocarcinoma, Int. J. Gynecol. Pathol. 31 (2012) 304–312.

[26] R. Brosh, V. Rotter, When mutants gain new powers: news from the mutant p53 field, Nat. Rev. Cancer 9 (2009) 701–713.

[27] O. Fadare, I.L. Renshaw, S.X. Liang, Does the loss of ARID1A (BAF-250a) expression in endometrial clear cell carcinomas have any clinicopathologic significance? A pilot assessment, J. Cancer 3 (2012) 129–136.

[28] Mclntyre JB, Nelson GS, Ghatage P, Morris D, Duggan MA, Lee CH, at el. PIK3CA missense mutation is associated with unfavorable outcome in grade 3 endometrioid carcinoma but not in serous endometrial carcinoma. Gynecol. Oncol. 2014; 132: 188–193.

[29] Y. Jin, Y. Li, L. Pan, The target therapy of ovarian clear cell carcinoma, Onco Targets Ther. 7 (2014) 1647–1652.

[30] T. Sato, D.E. Stange, M. Ferrante, R.G. Vries, J.H. Van Es, S. Van den Brink, et al., Long-term expansion of epithelial organoids from human colon, adenoma, adenocarcinoma, and Barrett's epithelium, Gastroenterology 141 (2011) 1762–1772.

[31] K. Onuma, M. Ochiai, K. Orihashi, M. Takahashi, T. Imai, H. Nakagama, et al., Genetic reconstitution of tumorigenesis in primary intestinal cells, Proc. Natl. Acad. Sci.

U. S. A. 110 (2013) 11127–11132.

[32] J. Drost, R.H. van Jaarsveld, B. Ponsioen, C. Zimberlin, R. van Boxtel, A. Buijs, et al., Sequential cancer mutations in cultured human intestinal stem cells, Nature 521 (2015) 43–47.

[33] P.W. Chi, J. Yang, S.K. Ng, C. Feltmate, M.G. Muto, K. Hasselblatt, et al., Loss of E-cadherin disrupts ovarian epithelial inclusion cyst formation and collective movement in ovarian cancer cells, Oncotarget 7 (2016) 4110–4121.

[34] S. Mabuchi, C. Kawase, D.A. Altomare, K. Morishige, K. Sawada, M. Hayashi, et al., mTOR is a promising therapeutic target both in cisplatin-sensitive and cisplatin-resistant clear cell carcinoma of the ovary, Clin. Cancer Res. 15 (2009) 5404–5413.

[35] B.G. Bitler, K.M. Aird, A. Garipov, H. Li, M. Amatangelo, A.V. Kossenkov, et al., Synthetic lethality by targeting EZH2 methyltransferase activity in ARID1A-mutated cancers, Nat. Med. 21 (2015) 231–238.

[36] L.B. Alexandrov, S. Nik-Zainal, D.C. Wedge, S.A. Aparicio, S. Behjati, A.V. Biankin, et al., Signatures of mutational processes in human cancer, Nature 500 (2013) 415–421.

[37] Integrated genomic analyses of ovarian carcinoma. Cancer genome atlas network,

Nature 474 (2011) 609–615.

[38] Y. Uehara, K. Oda, Y. Ikeda, T. Koso, S. Tsuji, S. Yamamoto, et al., Integrated copy number and expression analysis identifies profiles of whole-arm chromosomal alterations and subgroups with favorable outcome in ovarian clear cell carcinomas, PLoS One 10 (2015), e0128066.

[39] C. Williams, F. Ponten, C. Moberg, P. Söderkvist, M. Uhlén, J. Pontén, et al., A high frequency of sequence alterations is due to formalin fixation of archival specimens, Am. J. Pathol. 155 (1999) 1467–1471.

[40] M. Srinivasan, D. Sedmak, S. Jewell, Effect of fixatives and tissue processing on the content and integrity of nucleic acids, Am. J. Pathol. 161 (2002) 1961–1971.

pted for NGS analysis. If either template DNA of 5 ng or 20 ng has passed the quality check, NGS analysis has been performed.

Table 1

Table 1 Clinico-pathologic features of enrolled 29 OCCC cases and 18 cases which passed DNA quality control testing

Characteristics	Data	
	All	QC passed
Number of cases	29	18
Median age (range)	54 (40-74)	55 (41-71)
Site of primary tumor, right/left	16/13	9/9
Histological diagnoses		
Clear cell adenocarcinoma	26	16
Clear cell adenocarcinofibroma	1	1
Clear cell adenocarcinoma + Endometrioid adenocarcinoma	2	1
Lymph node metastasis, with/without/unknown	2/25/2	2/15/1
Endometriosis, with/without	19/10	13/5
FIGO staging		
I	20	12
II	3	3
III	3	2
IV	3	1

Table 2

Table 2 Clinico-pathologic features of 29 OCCCs and summary of somatic mutations identified from 18 OCCCs sequenced by the NGS analysis

Case No.	Age	Endometriosis	Tumor Site	FIGO staging	TNM stage	Histology	Fixation time	Storage time points of FFPE	QC	NGS No.	Somatic mutations identified (nonsynonymous)	Prognosis
1	40	Yes	Right	IV	T2cN0M1	CCC+EMC	Over 24 h	36-48 months	Not passed			Dead
2	66	No	Left	Ia	T1aN0M0	CCC	< 24 h	24-36 months	Not passed			Alive
3	52	Yes	Right	Ia	T1aN0M0	CCC	< 24 h	24-36 months	Not passed			Dead
4	59	No	Right	Ic	T1cN0M0	CCC	< 24 h	24-36 months	Not passed			Alive
5	52	Yes	Left	Ic	T1cN0M0	CCC	< 24 h	24-36 months	Not passed			Alive
6	47	No	Left	Ia	T1aN0M0	CCC	Over 24 h	24-36 months	Not passed			Alive
7	73	Yes	Left	Ia	T1aN0M0	CCC	< 24 h	24-36 months	Not passed			Alive
8	74	No	Right	IIIb	T3bN0M0	CCC	< 24 h	24-36 months	Not passed			Dead
9	60	Yes	Left	Ia	T1aN0M0	CCC	< 24 h	24-36 months	Passed	#9	PKHD1, CRTC1	Alive
10	51	Yes	Right	IV	T1aN1M1	CCC	Over 24 h	12-24 months	Not passed			Alive
11	69	No	Right	IIc	T2cN0M0	CCC	Over 24 h	12-24 months	Passed	#3	BCL6, ETS1, WAS	Alive
12	52	Yes	Left	Ic	T1cN0M0	CCC+EMC	< 24 h	12-24 months	Passed	#4	CTNNB1, TP53, PAK3	Alive
13	63	No	Right	Ia	T1aN0M0	CCC	< 24 h	12-24 months	Passed	#5	MDM4, PIK3CA	Alive
14	44	Yes	Right	IIIc	T1aN1M0	CCCF	< 24 h	12-24 months	Passed	#6	PDE4DIP, TP53	Alive
15	56	Yes	Right	Ia	T1aN0M0	CCC	< 24 h	1-12 months	Not passed			Alive
16	69	No	Right	Ic	T1cN0M0	CCC	< 24 h	1-12 months	Not passed			Alive
17	71	Yes	Left	IIc	T2cN0M0	CCC	< 24 h	1-12 months	Passed	#1	SYNE1, PIK3CG	Alive
18	55	Yes	Right	Ia	T1aN0M0	CCC	< 24 h	1-12 months	Passed	#2	NFE2L2, PTCH1	Alive
19	56	No	Right	Ia	T1aN0M0	CCC	< 24 h	1-12 months	Passed	#7	LRP1B, SF3B1, LIFR	Alive
20	46	No	Left	IV	T1cN1M1	CCC	< 24 h	1-12 months	Passed	#8	BAI3	Alive
21	57	Yes	Left	Ic	T1cNxM0	CCC	< 24 h	1-12 months	Passed	#10	CSMD3	Alive
22	53	Yes	Left	Ic	T1cN0M0	CCC	Over 24 h	1-12 months	Passed	#11	PIK3CA	Alive
23	54	No	Left	IIIa	T3aN0M0	CCC	< 24 h	1-12 months	Passed	#12	MAG1, PIK3CA, CSMD3, TLR4, PIK3R2, AMER1	Alive
24	41	Yes	Right	IIc	T2cN0M0	CCC	< 24 h	1-12 months	Passed	#13	FBXW7	Alive
25	45	Yes	Right	Ic	T1cN0M0	CCC	< 24 h	1-12 months	Passed	#14	ARID1A, LRP1B, SMARCA4, PPP2R1A	Alive
26	56	Yes	Right	Ia	T1aN0M0	CCC	< 24 h	1-12 months	Passed	#15	CTNNB1, LPHN3	Alive
27	50	Yes	Right	Ic	T1cN0M0	CCC	< 24 h	1-12 months	Passed	#16	ARID1A, PIK3CA, DST, NUMA1, ERBB2	Alive
28	51	Yes	Left	Ic	T1cN0M0	CCC	< 24 h	1-12 months	Passed	#17	ARID1A, LPHN3, KDM5C	Alive
29	61	Yes	Left	Ia	T1aN0M0	CCC	< 24 h	1-12 months	Passed	#18	PIK3CA, PTEN	Alive

CCC, clear cell adenocarcinoma; CCCF, clear cell adenocarcinofibroma; EMC, endometrioid adenocarcinoma

Table 3

Table 3 A total of 7 genes were mutated in multiple OCCC cases

Sample no.	Gene	Position	Ref	Alt	Type of alteration	NM number	Protein change	Var (%)	Reads	Provean Prediction	SIFT Prediction	dbSNP ID	COSMIC ID
#5	PIK3CA	chr3:178951957	G	A	Missense	NM_006218	p.M1004I	32	3842	Deletrious	Damaging		COSM1420934
#11	PIK3CA	chr3:178936092	A	G	Missense	NM_006218	p.E545G	20	2007	Deletrious	Damaging	rs121913274	COSM764
#12	PIK3CA	chr3:178952085	A	G	Missense	NM_006218	p.H1047R	46	102	Neutral	Damaging	rs121913279	COSM775
#16	PIK3CA	chr3:178936082	G	A	Missense	NM_006218	p.E542K	27	1643	Neutral	Damaging	rs121913273	COSM760
#18	PIK3CA	chr3:178921555	T	G	Missense	NM_006218	p.V346G	23	120	Deletrious	Damaging		COSM4714415
#14	ARID1A	chr1:27057682	C	T	Nonsense	NM_139135	p.Q464X	55	1053	NA	NA		COSM5347142
#16	ARID1A	chr1:27057988	C	T	Nonsense	NM_139135	p.Q566X	41	215	NA	NA		COSM1296220
#17	ARID1A	chr1:27058093	C	T	Nonsense	NM_139135	p.Q601X	90	176	NA	NA		
#4	CTNNB1	chr3:41266101	C	G	Missense	NM_001098210	p.S33C	45	1067	Deletrious	Damaging	rs121913400	COSM5677
#15	CTNNB1	chr3:41266113	C	G	Missense	NM_001098210	p.S37C	39	810	Deletrious	Damaging	rs12193403	COSM5679
#10	CSMD3	chr8:113662521	C	T	Missense	NM_198123	p.R1021H	58	4830	Deletrious	Damaging		
#12	CSMD3	chr8:113421175	A	C	Missense	NM_198123	p.L1828V	30	1584	Deletrious	Tolerated		
#15	LPHN3	chr4:62598744	G	A	Missense	NM_015236	p.E223K	37	1460	Deletrious	Damaging		
#17	LPHN3	chr4:62863907	C	A	Missense	NM_015236	p.L1039I	41	225	Neutral	Damaging		
#7	LRP1B	chr2:141267618	T	C	Missense	NM_018557	p.I2759M	23	130	Neutral	Tolerated		
#14	LRP1B	chr2:142012102	C	T	Missense	NM_018557	p.R151K	10	516	Neutral	Tolerated		
#4	TP53	chr17:7578406	C	T	Missense	NM_001126115	p.R43H	10	1986	Deletrious	Damaging	rs28934578	COSM99023
#6	TP53	chr17:7579882	C	T	Missense	NM_001126112	p.E11K	40	2495	Neutral	Damaging		COSM3820734

Var (%): variant allele frequency

Table 4

Table 4 Summary of 45 somatic mutations in 34 genes were identified in 18 OCCCs

Sample no.	Gene	Position	Ref	Alt	Type of alteration	NM number	Protein change	Var (%)	Reads	Provean Prediction	SIFT Prediction	dbSNP ID	COSMIC ID
#1	SYNE1	shr6:152469215	T	G	Missense	NM_033071	p.K8243T	48	2714	Neutral	Tolerated		
#1	PIK3CG	chr7:106545584	C	T	Missense	NM_001282426	p.R1021C	40	5441	Deletrious	Damaging		COSM5698913
#2	NFE2L2	chr2:178098800	T	C	Missense	NM_006164	p.E82G	10	5067	Deletrious	Damaging		COSM132853
#2	PTCH1	chr9:98220390	G	A	Missense	NM_001083602	p.R959C	29	2538	Deletrious	Damaging		
#3	BCL6	chr3:187447314	G	C	Nonsense	NM_001134738	p.Y293X	38	3766	NA	NA		
#3	ETS1	chr11:128426292	C	T	Missense	NM_001143820	p.M36I	69	301	Neutral	Tolerated		
#3	WAS	chrX:48542310	C	T	Missense	NM_000377	p.P23L	35	675	Deletrious	Damaging		
#4	CTNNB1	chr3:41266101	C	G	Missense	NM_001098210	p.S33C	45	1067	Deletrious	Damaging	rs121913400	COSM5677
#4	TP53	chr17:7578406	C	T	Missense	NM_001126115	p.R43H	10	1986	Deletrious	Damaging	rs28934578	COSM99023
#4	PAK3	chrX:110463589	C	T	Missense	NM_001128167	p.P517S	34	812	Deletrious	Tolerated		
#5	MDM4	chr1:204518424	C	T	Nonsense	NM_002393	p.R363X	11	3274	NA	NA		
#5	PIK3CA	chr3:178951957	G	A	Missense	NM_006218	p.M1004I	32	3842	Deletrious	Damaging		COSM1420934
#6	PDE4DIP	chr1:145075777	G	A	Missense	NM_022359	p.T29M	15	1368	Neutral	Damaging		
#6	TP53	chr17:7579882	C	T	Missense	NM_001126112	p.E11K	40	2495	Neutral	Damaging		COSM3820734
#7	LRP1B	chr2:141267618	T	C	Missense	NM_018557	p.I2759M	23	130	Neutral	Tolerated		
#7	SF3B1	chr2:198267361	T	G	Missense	NM_012433	p.K666Q	37	1130	Deletrious	Damaging		COSM132950
#7	LIFR	chr5:38482184	C	T	Missense	NM_002310	p.R936H	25	422	Neutral	Tolerated		
#8	BAI3	chr6:69349139	T	C	Missense	NM_001704	p.I191T	37	1123	Deletrious	Damaging		
#9	PKHD1	chr6:51618148	C	A	Missense	NM_138694	p.S2934I	44	1167	Deletrious	Damaging		
#9	CRTC1	chr19:18856739	G	A	Missense	NM_015321	p.R117Q	11	198	Neutral	Damaging		
#10	CSMD3	chr8:113662521	C	T	Missense	NM_198123	p.R1021H	58	4830	Deletrious	Damaging		
#11	PIK3CA	chr3:178936092	A	G	Missense	NM_006218	p.E545G	20	2007	Deletrious	Damaging	rs121913274	COSM764
#12	MAGI1	chr3:65350349	T	A	Missense	NM_001033057	p.Q1114H	33	457	Neutral	Tolerated		
#12	PIK3CA	chr3:178952085	A	G	Missense	NM_006218	p.H1047R	46	102	Neutral	Damaging	rs121913279	COSM775
#12	CSMD3	chr8:113421175	A	C	Missense	NM_198123	p.L1828V	30	1584	Deletrious	Tolerated		
#12	TLR4	chr9:120476450	A	C	Missense	NM_003266	p.S642R	32	3324	Deletrious	Damaging		
#12	PIK3R2	chr19:18277102	G	C	Missense	NM_005027	p.E517Q	36	1571	Deletrious	Damaging		
#12	AMER1	chrX:63412694	T	G	Missense	NM_152424	p.K158T	36	75	Neutral	Damaging		COSM287151
#13	FBXW7	chr4:153249385	G	A	Missense	NM_018315	p.R385C	26	11650	Deletrious	Damaging		COSM170725
#14	ARID1A	chr1:27057682	C	T	Nonsense	NM_139135	p.Q464X	55	1053	NA	NA		COSM5347142
#14	LRP1B	chr2:142012102	C	T	Missense	NM_018557	p.R151K	10	516	Neutral	Tolerated		
#14	SMARCA4	chr19:11096976	G	T	Missense	NM_003072	p.G156V	27	156	Neutral	Damaging		
#14	PPP2R1A	chr19:52715982	C	T	Missense	NM_014225	p.R183W	61	2937	Deletrious	Damaging		COSM51211
#15	CTNNB1	chr3:41266113	C	G	Missense	NM_001098210	p.S37C	39	810	Deletrious	Damaging	rs12193403	COSM5679
#15	LPHN3	chr4:62598744	G	A	Missense	NM_015236	p.E223K	37	1460	Deletrious	Damaging		
#16	ARID1A	chr1:27057988	C	T	Nonsense	NM_139135	p.Q566X	41	215	NA	NA		COSM1296220
#16	PIK3CA	chr3:178936082	G	A	Missense	NM_006218	p.E542K	27	1643	Neutral	Damaging	rs121913273	COSM760
#16	DST	chr6:56507439	C	T	Missense	NM_001723	p.E50K	34	1012	Neutral	Tolerated		
#16	NUMA1	chr11:71725554	G	A	Missense	NM_001286561	p.R999C	35	519	Deletrious	Damaging		COSM356705
#16	ERBB2	chr17:37880998	G	T	Missense	NM_001289937	p.G776V	27	748	Deletrious	Damaging		COSM18609
#17	ARID1A	chr1:27058093	C	T	Nonsense	NM_139135	p.Q601X	90	176	NA	NA		
#17	LPHN3	chr4:62863907	C	A	Missense	NM_015236	p.L1039I	41	225	Neutral	Damaging		
#17	KDM5C	chrX:53221934	G	A	Missense	NM_001146702	p.P1378S	41	4392	Neutral	Damaging		
#18	PIK3CA	chr3:178921555	T	G	Missense	NM_006218	p.V346G	23	120	Deletrious	Damaging		COSM4714415
#18	PTEN	chr10:89685307	T	C	Missense	NM_000314	p.Y68H	67	122	Deletrious	Damaging		COSM5036

Var (%): variant allele frequency

Figure 1

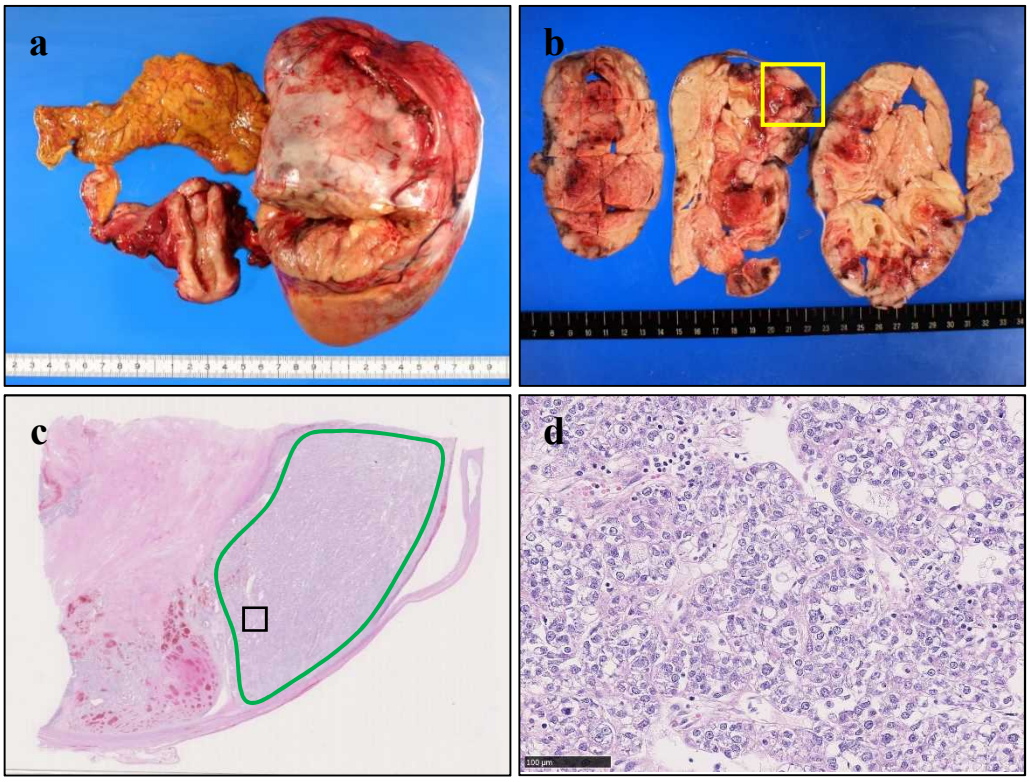

Figure 1 Representative images of OCCC for this study. (a, b) Macroscopic findings of left ovarian tumor. (c) Loupe image of region demarcated by the yellow square in b (hematoxylin & eosin staining). Area enclosed by green line is the macrodissected area. (d) Magnified image of the region represented by the black square in c. Tumor cells with abundant clear or eosinophilic cytoplasm. The scale bar is 100 μm.

Figure 2

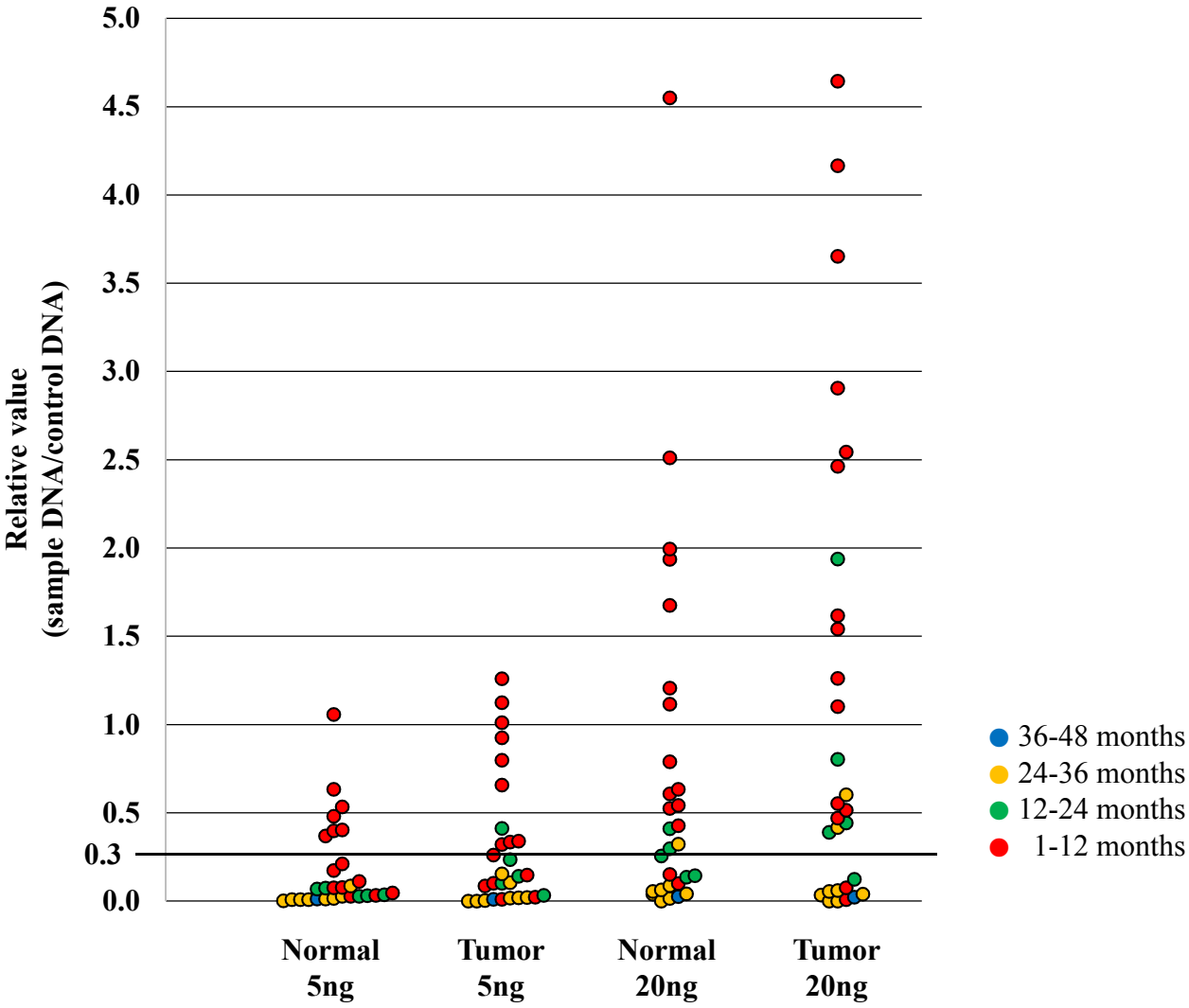

Figure 2 A dot blot of the distribution of quality of each DNA sample extracted from FFPE samples of 29 cases, which was evaluated by the qPCR method, is shown. Cases with relative value of > 0.3 are depicted a bold horizontal line. Both tumor and normal samples above this line are basically accepted for NGS analysis. If either template DNA of 5 ng or 20 ng has passed the quality check, NGS analysis has been performed.

Figure 3

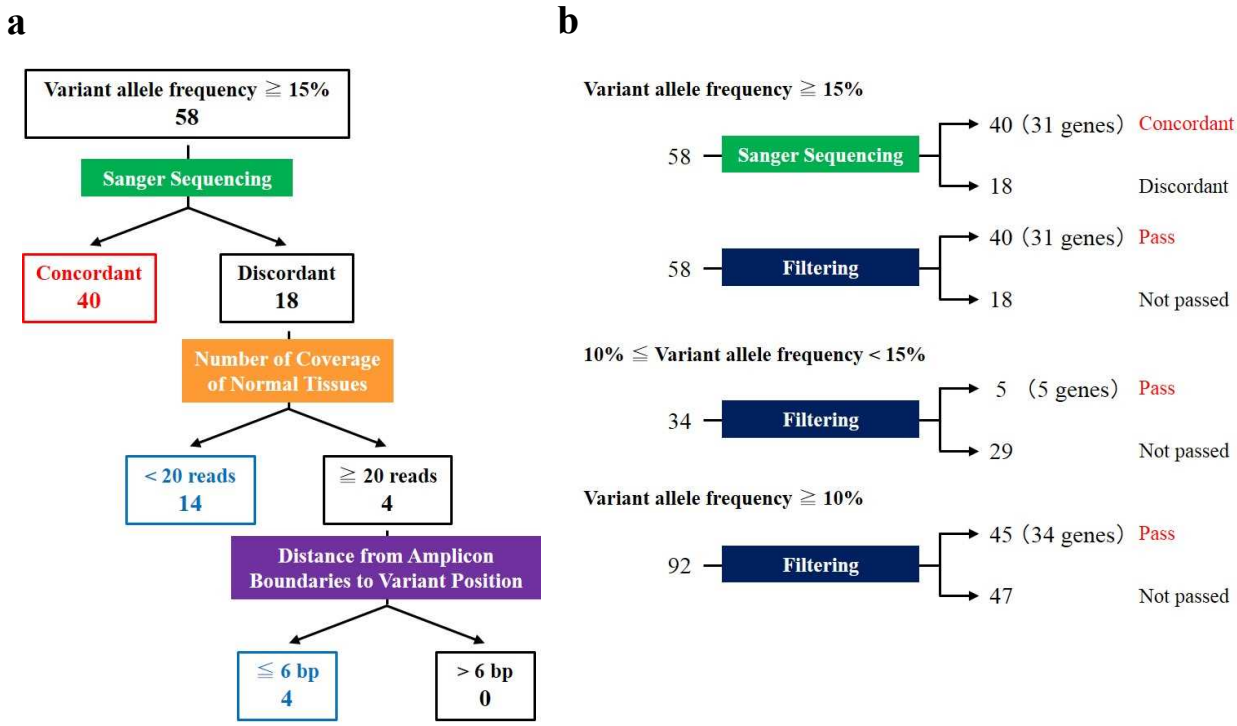

Figure 3 (a) A chart presents the validation by Sanger sequencing for 58 candidate somatic mutations with > 15% variant allele frequency. (b) Filtering of NGS data. Filtering conditions are > 20 reads in normal tissues and > 6 bp distance from amplicon boundaries to variant position. All tumor samples have reached sequencing coverage of > 50 reads.

Figure 4

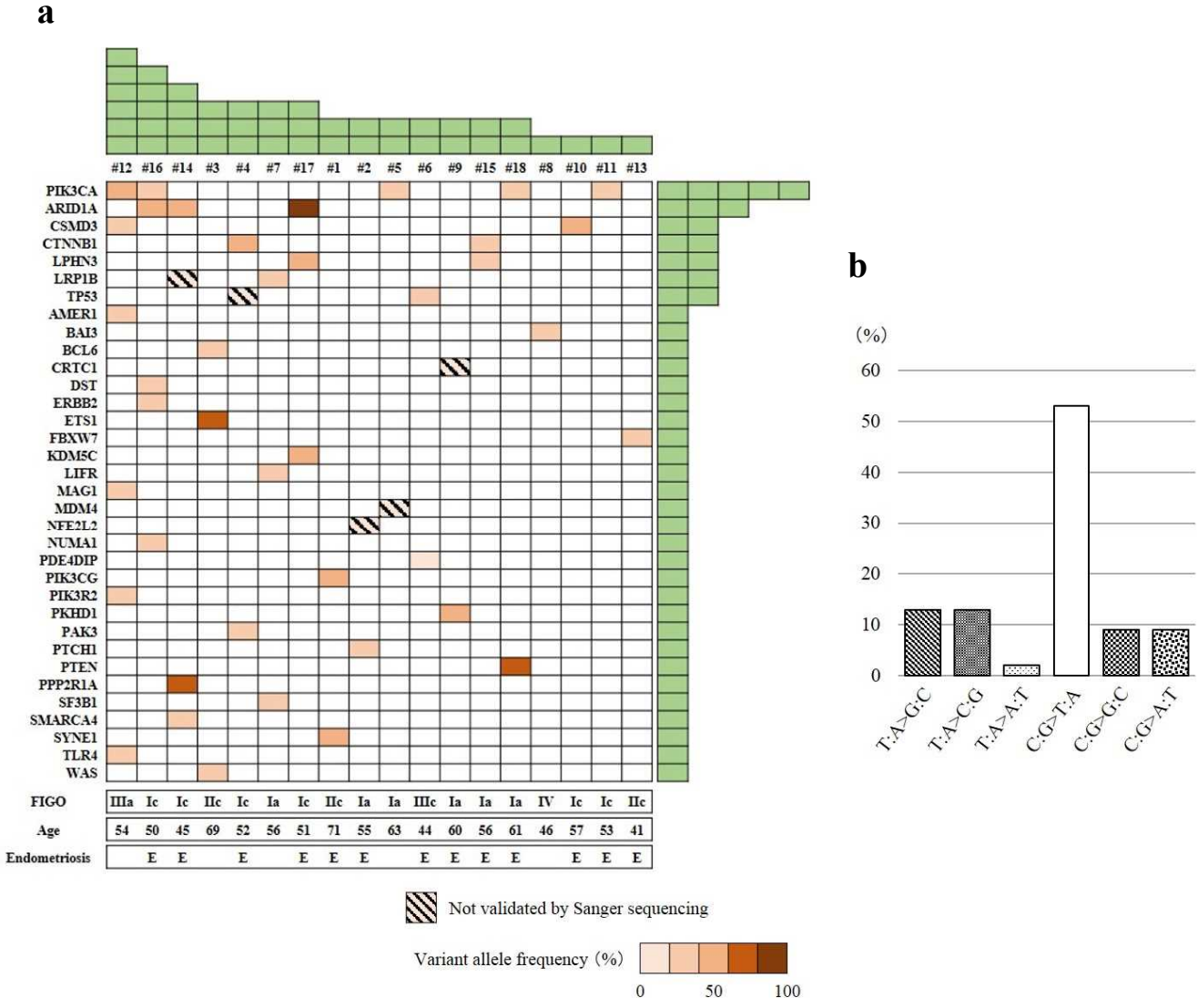

Figure 4 A summary of 45 somatic mutations identified by NGS analysis for 409 cancer-related genes in 18 OCCC samples is shown. (a) Forty five somatic mutations have been identified in 34 genes. Variant allele frequency is indicated according to the color scale. The number of variants is indicated the cumulative number of green boxes. (b) A bar graph represents the DNA substitution of 45 somatic mutations found in OCCC.

Figure 5

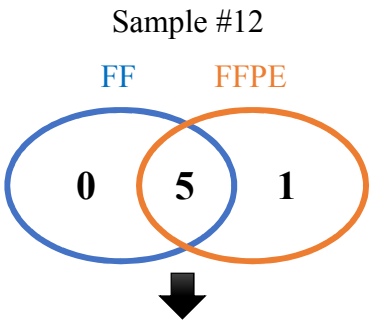

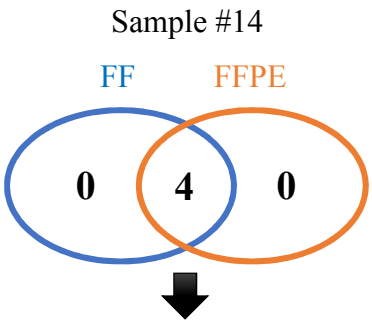

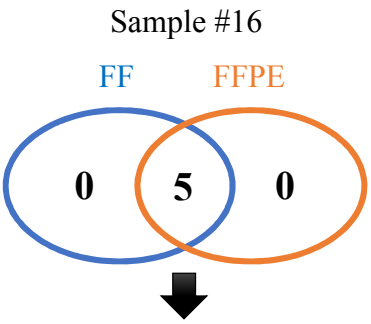

Variant allele frequency

	FF	FFPE
AMER1	0%	36%
CSMD3	36%	30%
MAGI1	31%	33%
PIK3CA	50%	46%
PIK3R2	35%	36%
TLR4	27%	32%

Variant allele frequency

	FF	FFPE
ARID1A	59%	55%
LRP1B	11%	10%
SMARCA4	28%	27%
PPP2R1A	63%	61%

Variant allele frequency

	FF	FFPE
ARID1A	24%	41%
ERBB2	22%	27%
DST	20%	34%
NUMA1	28%	35%
PIK3CA	16%	27%

Figure 5 A comparative representations between FFPE and FF-based NGS data from three OCCC cases.

Figure 6

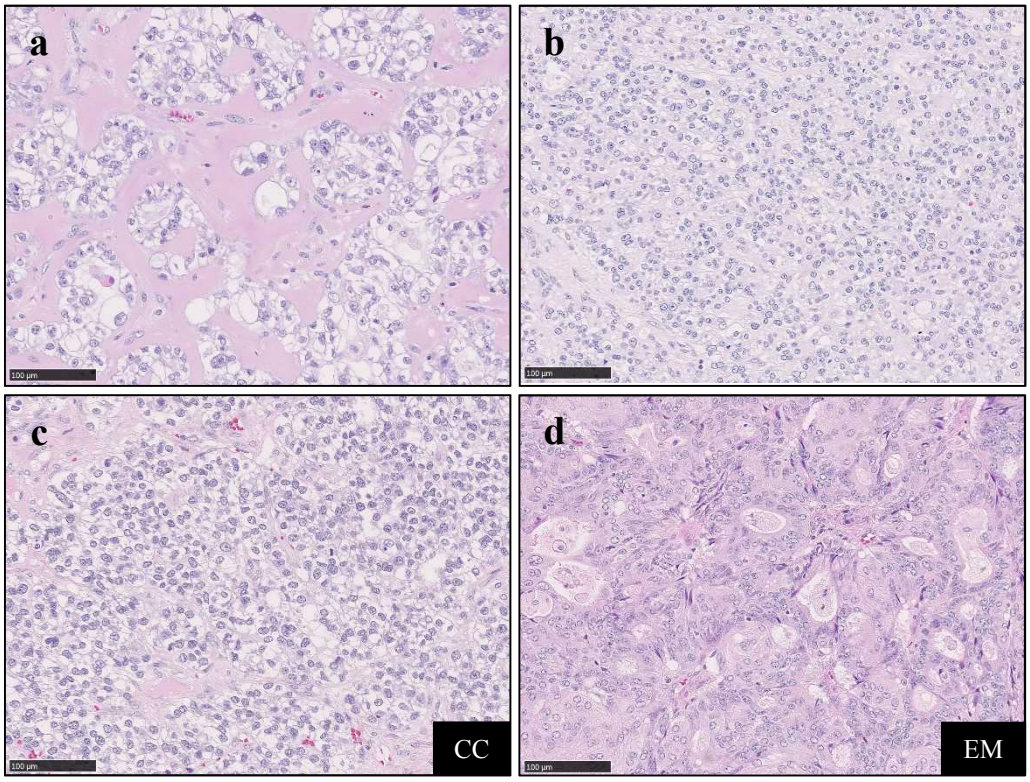

Figure 6 Variable histological features of OCCC cases. Each component was macrodissected from unstained FFPE sections for NGS. (a, b) Case #15 showing variable morphologies of OCCC. (a) Tumor cells with abundant eosinophilic basement membrane like material. (b) Tumor with solid growth. (c, d) Case #4 showing mixed epithelial tumors. (c) and (d) are clear cell adenocarcinoma (CC) and endometrioid adenocarcinoma (EM), respectively. The scale bar is 100 μm.

Gynecologic Oncology Vol. 144 Issue 2 p. 377-383
平成 29 年 2 月　　公表済